AD-A187 055 HIGH-FREQUENCY RADIOWAVE PROBING OF THE HIGH-LATITUDE IONOSPHERE(U) JOHNS HOPKINS UNIV LAUREL MD APPLIED PHYSICS LAB R A GREENWALD 1985 AFOSR-TR-87-1469 1/1

UNCLASSIFIED AFOSR-86-0028 F/G 20/14 NL

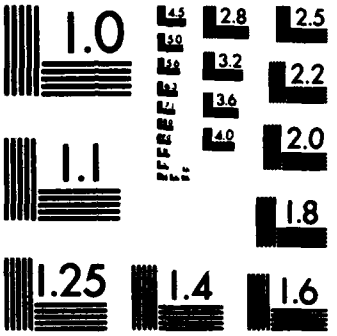

MICROCOPY RESOLUTION TEST CHART
NATIONAL BUREAU OF STANDARDS-1963-A

DTIC FILE COPY

DISTRIBUTION STATEMENT A
Approved for public release;
Distribution Unlimited

(2)

AD-A187 055

REPORT DOCUMENTATION PAGE

Form Approved OMB No. 0704-0188

1b. RESTRICTIVE MARKINGS

2a. SECURITY CLASSIFICATION AUTHORITY

2b. DECLASSIFICATION / DOWNGRADING SCHEDULE

3. DISTRIBUTION / AVAILABILITY OF REPORT
Approved for public release;
Distribution unlimited.

4. PERFORMING ORGANIZATION REPORT NUMBER(S)

5. MONITORING ORGANIZATION REPORT NUMBER(S)
AFOSR-TR- 87-1469

6a. NAME OF PERFORMING ORGANIZATION
Johns Hopkins University

6b. OFFICE SYMBOL (If applicable)

7a. NAME OF MONITORING ORGANIZATION
AFOSR/NC

DTIC ELECTE NOV 0 9 1987 S D H

6c. ADDRESS (City, State, and ZIP Code)
Applied Physics Laboratory
Laurel, MD 20707

7b. ADDRESS (City, State, and ZIP Code)
Building 410
Bolling AFB
DC 20332-6448

8a. NAME OF FUNDING / SPONSORING ORGANIZATION
AFOSR

8b. OFFICE SYMBOL (If applicable)
NC

9. PROCUREMENT INSTRUMENT IDENTIFICATION NUMBER
AFOSR-ISSA-86-0028

8c. ADDRESS (City, State, and ZIP Code)
Building 410
Bolling AFB
DC 20332-6448

10. SOURCE OF FUNDING NUMBERS

PROGRAM ELEMENT NO.	PROJECT NO.	TASK NO	WORK UNIT ACCESSION NO.
61102F	2310	A2	

11. TITLE (Include Security Classification)
HIGH-FREQUENCY RADIOWAVE PROBING OF THE HIGH-LATITUDE IONOSPHERE

12. PERSONAL AUTHOR(S)
Raymond A. Greenwald

13a. TYPE OF REPORT
Reprint

13b. TIME COVERED
FROM ________ TO ________

14. DATE OF REPORT (Year, Month, Day)

15. PAGE COUNT

16. SUPPLEMENTARY NOTATION

17. COSATI CODES

FIELD	GROUP	SUB-GROUP

18. SUBJECT TERMS (Continue on reverse if necessary and identify by block number)

Original contains color plates: All DTIC reproductions will be in black and white

Accession For
NTIS GRA&I ☑
DTIC TAB ☐
Unannounced ☐
Justification
By
Distribution/
Availability Codes
Dist | Avail and/or Special
A-1 | 20

DTIC COPY INSPECTED

19. ABSTRACT (Continue on reverse if necessary and identify by block number)

During the past several years, a program of high-frequency radiowave studies of the high-latitude ionosphere has been developed ~~in the APL Space Department~~. Studies are now being conducted on the formation and motion of high-latitude ionospheric electron density irregularities, using a sophisticated high-frequency radar system installed at Goose Bay, Labrador. The radar antenna is also being used to receive signals from a beacon transmitter located at Thule, Greenland. This information is providing a better understanding of the spatial and temporal variability of high-latitude propagation channels and their relationship to disturbances in the magnetosphere-ionosphere system.

20. DISTRIBUTION / AVAILABILITY OF ABSTRACT
☒ UNCLASSIFIED/UNLIMITED ☒ SAME AS RPT ☐ DTIC USERS

21. ABSTRACT SECURITY CLASSIFICATION
Unclassified

22a. NAME OF RESPONSIBLE INDIVIDUAL
JAMES P. KOERMER, Lt Col, USAF

22b. TELEPHONE (Include Area Code)
(202) 767-4960

22c. OFFICE SYMBOL
NC

DD Form 1473, JUN 86 Previous editions are obsolete. SECURITY CLASSIFICATION OF THIS PAGE

RAYMOND A. GREENWALD

HIGH-FREQUENCY RADIOWAVE PROBING OF THE HIGH-LATITUDE IONOSPHERE 1985

During the past several years, a program of high-frequency radiowave studies of the high-latitude ionosphere has been developed in the APL Space Department. Studies are now being conducted on the formation and motion of high-latitude ionospheric electron density irregularities, using a sophisticated high-frequency radar system installed at Goose Bay, Labrador. The radar antenna is also being used to receive signals from a beacon transmitter located at Thule, Greenland. This information is providing a better understanding of the spatial and temporal variability of high-latitude propagation channels and their relationship to disturbances in the magnetosphere-ionosphere system.

INTRODUCTION

At altitudes above 100 kilometers, the atmosphere of the earth gradually changes from a predominantly neutral medium to an increasingly ionized gas or plasma. The ionization is caused chiefly by a combination of solar extreme ultraviolet radiation and, at high latitudes, particle precipitation from the earth's magnetosphere. Because of its ionized nature between 100 and 1000 kilometers, this part of the atmosphere is commonly referred to as the ionosphere. In this region, typically below an altitude of 400 kilometers, the ionosphere can refract radio waves and enable long-distance radio communication in the high-frequency (HF) spectrum. While the satellite era has reduced the need for this type of communication to some degree, there are still many applications, including aircraft and shipboard communication, in which long-distance radio communication via ionospheric paths remains important. For these, HF communication (3 to 30 megahertz) is typically the band of choice.

In addition to its usefulness as a communication medium, the HF frequency band is also being considered for use in surveillance radars. Here the advantage lies in the ionospheric path, which extends the range of potential target detection from approximately 100 kilometers to several thousand kilometers.

At low and middle latitudes, HF radiowave systems operate quite successfully. The ionosphere is produced predominantly by extreme ultraviolet radiation, and one is generally able to predict optimum HF operating frequencies over the course of a day. However, at high latitudes, magnetospheric particle precipitation plays a major role in producing the ionosphere. We know that precipitation occurs as a result of disturbances in the earth's magnetosphere-ionosphere system, which, in turn, are related to disturbances in the solar wind impinging on the earth's magnetosphere. Unfortunately, the interactions between the solar wind, the magnetosphere, and the ionosphere are not totally understood, and our ability to detect solar wind disturbances prior to their impingement on the magnetosphere is quite limited. Therefore, we still have only limited success in forecasting sudden changes in the high-latitude ionosphere and consequently in high-latitude radiowave propagation.

In order for space scientists to obtain a better understanding of the various interactions occurring among the solar wind, the magnetosphere, and the ionosphere, active measurement programs are conducted in all three regions. The solar wind and magnetosphere measurements are made mainly from satellites. High-latitude ionospheric measurements use a variety of techniques, including remote sensing with ground-based radars. Radar studies include ionospheric sounding of electron density profiles,[1] incoherent scatter observations of the thermal plasma,[2] and coherent scatter observations of small-scale ionospheric structure.[3,4] Generally, coherent scatter studies have been performed with very high frequency (VHF) 30 to 300 megahertz and ultrahigh frequency (UHF) 300 to 3000 megahertz radars, which are essentially unaffected by changes in ionospheric properties.[3,4] However, in recent years there has been an extension of these studies toward lower frequencies that lie within the HF band,[5,6] a change that has enabled coherent scatter studies to be extended to higher latitudes and altitudes. Moreover, it has brought about the interesting situation that a radiowave system that is profoundly affected by high-latitude ionospheric disturbances is being used to provide a better understanding of their cause and nature. APL has been a world leader in this effort, and this article presents a synopsis of its achievements to date.

WHY HF RADARS?

Ionospheric irregularity structures may be produced at both high and low latitudes, over a range of altitudes, and by a variety of mechanisms.[7,8,9] Nevertheless, all of these structures share a common tendency to be extended and aligned along the local magnetic

field. This alignment occurs because the magnetic force confines the ionospheric electron motion perpendicular to the magnetic field to cyclotron orbits of diameters that are typically less than a few centimeters; along the magnetic field lines, the electrons can expand much more freely, being restricted only by the electrostatic force of the more slowly moving ions. Therefore, the irregularities eventually assume an elongated shape and alignment with the field.

One can think of the irregularities as resembling a random distribution of needles that are aligned with the earth's magnetic field. It is clear that they will present the greatest radar cross section when they are viewed perpendicular to their axes. Moreover, when they are illuminated from an oblique angle, Snell's Law predicts that they will scatter the radar signals away from the radar site. This analogy has been extended in Fig. 1 to the real high-latitude world, where the irregularities are aligned with a magnetic field that is nearly vertical. The irregularities most commonly occur in two regions of the ionosphere: the E region at an altitude of 100 kilometers and the F region at an altitude of 300 kilometers. Signals from a VHF radar propagate in straight lines and are obliquely incident on the irregularity structures. A portion of the incident energy is scattered by the irregularities; however, as it scatters in accordance with Snell's Law, the scattered signals travel off into space. They might be seen by a satellite, but never by a ground-based radar. Such considerations limit ground-based VHF and UHF radars from observing both the E-region irregularities if the radars are located poleward of 60° magnetic latitude and the high-latitude F-region irregularities regardless of the radar location.

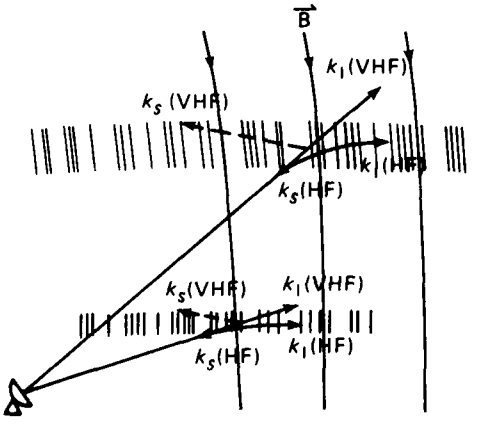

Figure 1—Illustration of the manner in which VHF and higher frequency radar signals are scattered into space by very-high-latitude E- and F-region electron density irregularities. At HF frequencies, the radar signals are refracted toward the horizontal as they enter those two ionospheric layers. If the signals are propagating perpendicular to the magnetic field lines when they encounter a region of irregularities, the backscattered signals will return to the radar.

Let us now consider the operation of an HF radar. At the lower frequencies, the radar signals are influenced by the ionosphere to a much greater extent. The dominant effect is for the signals to be refracted toward the horizontal as they enter ionospheric layers with higher electron density. While being refracted, the signals pass through a region in which they are propagating perpendicular to the magnetic field. If this region contains ionospheric irregularities, the radar signals will be backscattered and will return to the radar site. One need only choose an operating frequency that will result in propagation of the radar signal in the direction perpendicular to the magnetic field in the region of interest.

The operation of an over-the-horizon HF radar is a simple extension of this concept. For HF radars, the frequency is selected so that the signal is refracted by the ionosphere and returns to the ground at a great distance. There, a target such as an airplane might scatter the signal, which would return via the reciprocal ionospheric path to the radar. Unfortunately, HF antennas tend to have broad vertical patterns. Thus it is entirely possible that one will simultaneously receive weak signals caused by backscatter from a desired target and strong clutter signals caused by ionospheric irregularities.

HISTORY OF APL'S HF RADAR

The present APL HF radar effort began in the fall of 1981 through the support of the APL Independent Research and Development (IR&D) Program. At that time, there was a significant shift of research interest toward understanding both the interactions between the very-high-latitude ionosphere and the magnetosphere, and the formation, dispersion, and decay of electron density irregularities in the ionosphere. Two manifestations of this interest have been the movement of a large U.S. incoherent scatter radar facility to Sondre Stromfjord, Greenland, and the construction of the HILAT satellite (see the April-June 1984 issue of the *Johns Hopkins APL Technical Digest*). It was felt that this very-high-latitude research effort could be supported by an appropriately designed coherent scatter radar system. As discussed above, VHF or UHF facilities could not be used, but an HF radar appeared appropriate. The IR&D funds were used to develop a microcomputer-based radar controller and a phase-coherent radar receiver; subsequently, a unique broadband antenna phasing matrix and a complete software operating system for the radar were produced.

At about the same time, funding was received from the National Science Foundation to use one of their HF ionospheric sounders to perform coherent scatter radar observations in Alaska. The effort was unsuccessful and finally required the use of the IR&D prototype to obtain an adequate set of measurements. Subsequent analysis of the data demonstrated the potential value of the HF radar technique for high-latitude ionospheric studies and resulted in additional support from the National Science Foundation, the Air

Force Office of Scientific Research, the Defense Nuclear Agency, and the Air Force Geophysics Laboratory for the establishment of the present HF radar facility at Goose Bay, Labrador. Operation of the Goose Bay radar began in October 1983. Recently, additional support has been provided by the Rome Air Development Center for using the receiving portion of the Goose Bay facility to perform a detailed study of very-high-latitude HF propagation. Toward that end, fundamental improvements are being made in the HF antenna array. The modified antenna, which will also improve the radar capabilities of the facility, became operational in the autumn of 1984.

DESCRIPTION OF THE APL RADAR

APL's HF radar at Goose Bay, an auroral zone location, is at 65° geomagnetic latitude. The field of view of the radar is a large area extending over a 54° azimuth sector and covers 300 to 2400 kilometers in range. The azimuth sector is centered 2° to the east of geographic north, and the viewing area covers a portion of northeastern Canada and of Greenland. Figure 2 indicates this field of view as it is broken down into the 16 viewing directions of the radar. The small dark region along one of the directions represents the typical resolution cell of the radar. Also shown in the figure are the viewing area of a similar French radar (now under development) that will be used in conjunction with the Goose Bay radar to provide common volume measurements from two directions (shaded region), and the viewing areas of two incoherent scatter radars that are being used for collaborative studies (circles).

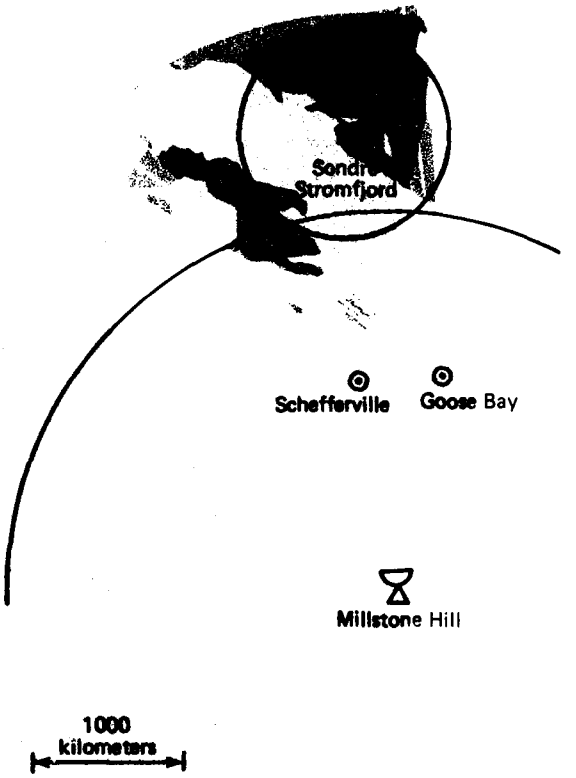

Figure 2—Field of view of APL's HF radar at Goose Bay. The radar can be pointed electronically into any of 16 possible directions with a resolution cell defined by the small dark-shaded region along one of the beams. Also shown are the nominal fields of view of the Sondre Stromfjord and Millstone Hill incoherent scatter radars and the planned field of view (light-shaded) of a French HF radar that will be located at Schefferville, Quebec. The French radar will be quite similar to the Goose Bay radar; together, they will be used for two-component measurements of irregularity drift.

A schematic diagram of the radar is shown in Fig. 3. The radar layout consists of low power and control electronics in the station approximately 274 meters from the antenna array, a phasing matrix and array select electronics in a shed at the center of one of the antenna arrays, an antenna array for transmission and reception, and a second antenna array used only for reception. Currently, the power amplifiers feeding the transmitting antennas are each capable of 125 watts peak output power, providing a total output power from the array of 2 kilowatts and an effective radiated power of 200 kilowatts (the latter specification includes the gain of the antenna array). In the future, we hope to improve these specifications by increasing the output power of each amplifier to 2 kilowatts.

The most important element of the Goose Bay radar is its electronically steered phased-array antenna. Originally it consisted of a linear array of 16 log-periodic antennas used for both transmission and reception. The antennas operate over the frequency band from 8 to 20 megahertz. A second antenna array has recently been constructed 100 meters to the north of the original array and parallel to it. The second array will be used for reception in conjunction with the original array and will provide important information on the vertical angle of arrival of the returning signal. Each array is 240 meters long and 15 meters above ground. Figure 4 is a photograph of the original array. Phasing of the antenna is accomplished with the broadband phasing matrix shown schematically in Fig. 5. The principal elements of the phasing matrix are the eight branching networks noted as "phasing trees." On transmit, signals enter a tree from the receiver side and pass through a network of power dividers and selected lengths of coaxial cable that ultimately produce successive time delays among the signals at the outputs. On receive, signals enter the tree from the antenna side and are reciprocally combined into a composite signal. In this mode, signals that arrive at the antenna array from the direction in which the antenna is phased will undergo constructive interference

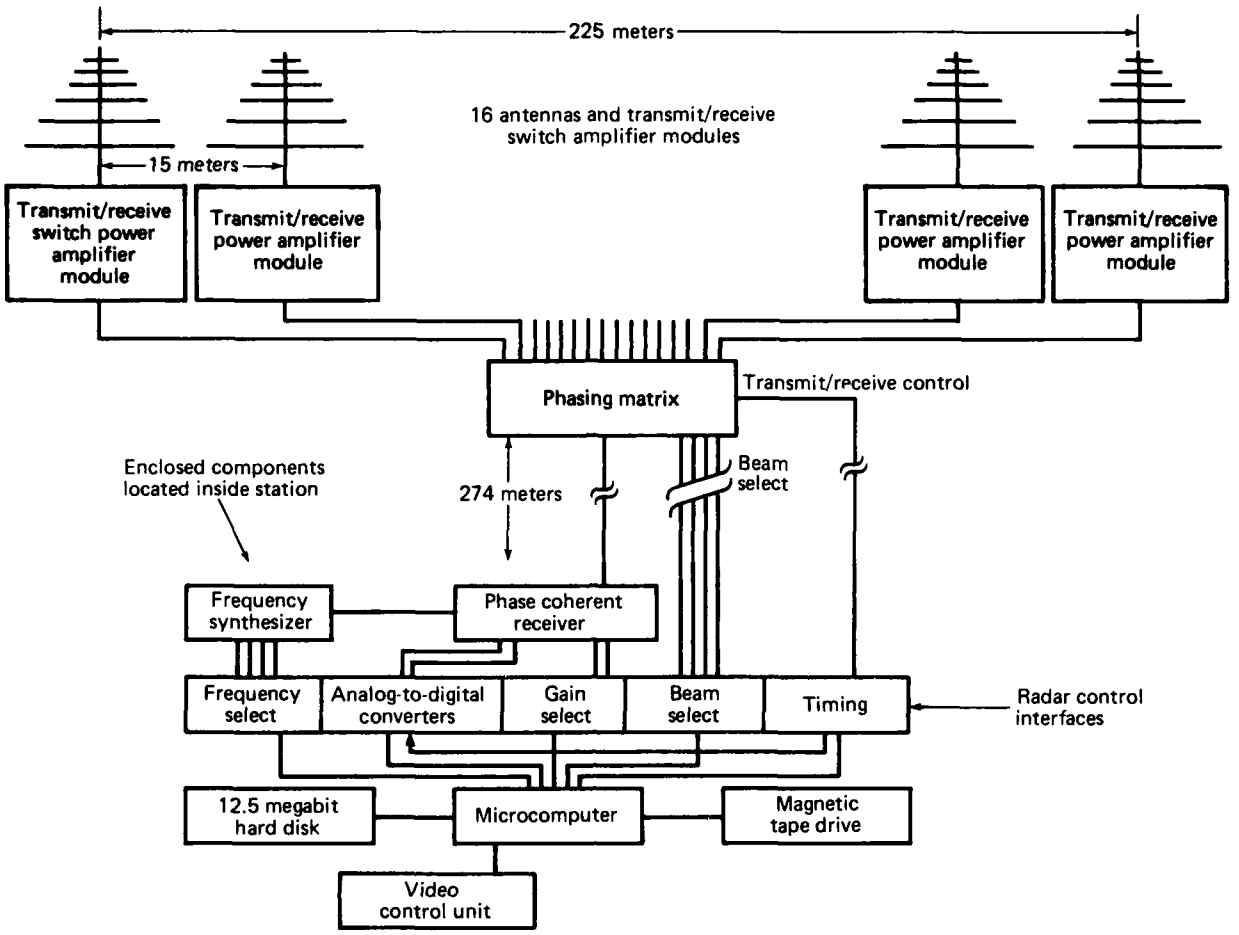

Figure 3—Schematic diagram of the APL radar as it existed prior to the installation of the new receive-only array. Each antenna is driven by a 125-watt broadband solid-state power amplifier located at the base of its support tower. Each power amplifier module also contains transmit/receive (T/R) switches for routing the transmitted and received power. The power supplies for the modules are located in the shed containing the phasing matrix at the center of the antenna array, and the remainder of the equipment is located in the station 274 meters from the center of the array.

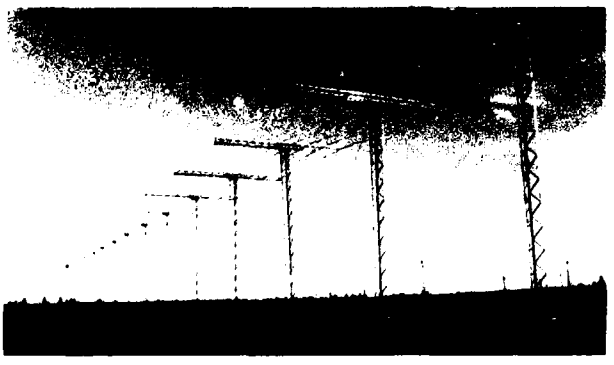

Figure 4—View of the original antenna array from the front, northwest corner. The shed containing the phasing matrix, array select logic, and power supplies is located at the center of the array.

within the phasing tree. The delay lines produce constant time delays through the phasing matrix. Therefore, the direction of any particular antenna beam is independent of frequency.

Each phasing tree produces one possible set of time delays across the antenna array. The 4-way switches shown in Fig. 5 are used to select one of the phasing trees, and the double-pole double-throw (crossover) switches are used to determine whether the selected beam is directed to the right or left of the array normal. The beam direction of the array can be switched in approximately 20 microseconds. The 16 possible beam azimuths range from 337° to 27°. The angular separation between beams is 3.3°, and the two-way antenna beamwidth varies from 2.5° at 20 megahertz to 6° at 8 megahertz.

Figure 6 exhibits several theoretical two-way azimuthal patterns of the eight beams directed to the right of the array normal. An additional eight beams with mirror-image patterns are directed to the left. Below 16 megahertz, the patterns do not exhibit any significant grating sidelobes, and other sidelobes are 27 decibels below the main lobe. Above 16 megahertz, grating sidelobes begin to appear for the outermost beams. That is, at 18 megahertz, beam 16 has a grating sidelobe at -44°, beam 15 has a grating sidelobe

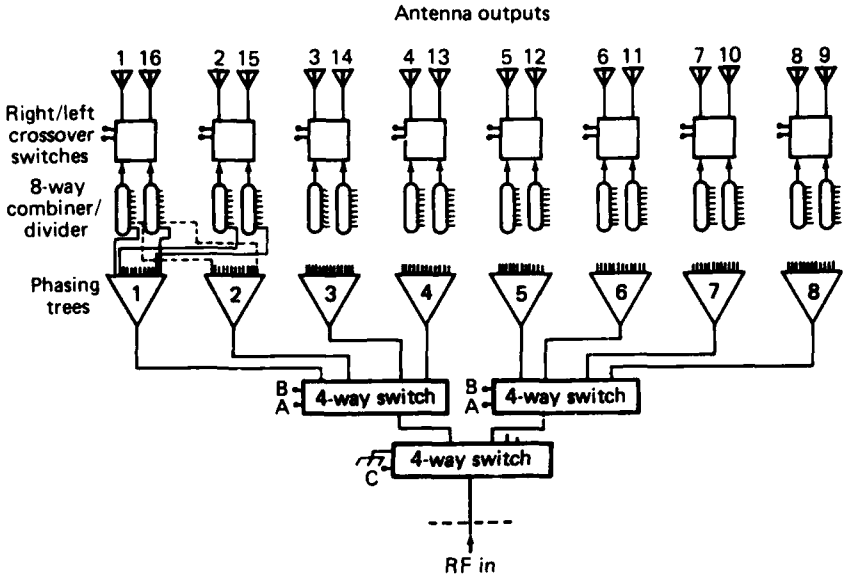

Figure 5—Schematic diagram of the phasing matrix, which establishes a progressive time delay across the antenna array on transmission and reforms the beam on reception. The 4-way switches select one of eight possible branching networks (phasing trees). Each tree consists of power dividers and delay lines that produce a specific time delay across the 16 outputs and represents one possible beam direction. The crossover switches determine whether the selected beam points to the right or left of the array normal. On reception, the process is reversed, and the matrix reinforces only those signals from the preselected direction.

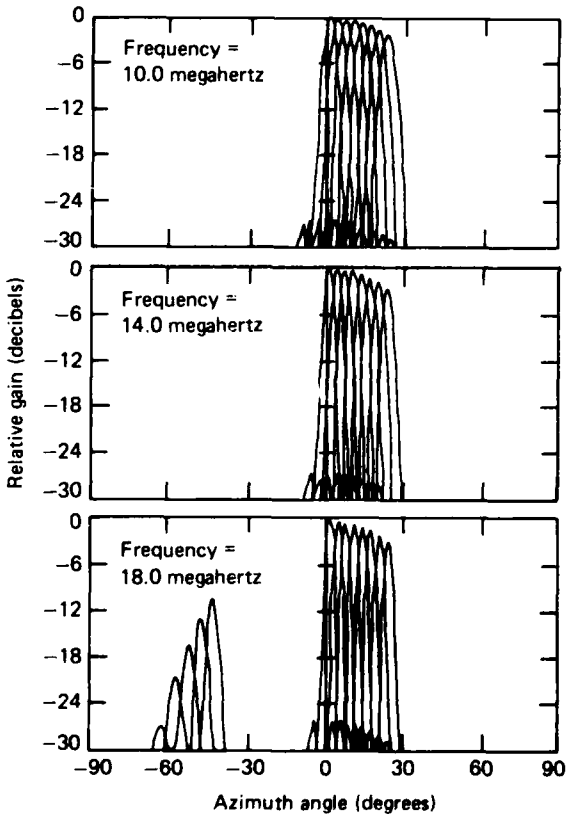

Figure 6—Theoretical two-way azimuthal patterns for eight lobes to the right of the array normal at frequencies of 10, 14, and 18 megahertz. Lobes at negative angles for the 18-megahertz case represent grating sidelobes of rightmost lobes. An additional mirror image set of patterns exists to the left of the array normal.

at -47.3°, and so on. To avoid the undesirable effects of these sidelobes, one might choose not to use these beams at the higher frequencies; however, we have not observed any ambiguities to date.

The vertical pattern of either of the arrays is quite broad, with an average half-power beamwidth of approximately 30°. At 8 megahertz, the vertical pattern maximum is at 35° elevation angle, whereas at 20 megahertz, it is at 15° elevation angle. Clearly, this broad coverage will not provide any significant information on the angle of arrival of the backscattered signal.

The advantage of having two receiving arrays will now be made clear. If we assume that one can measure the phase of the signal arriving at each of the arrays, the phase difference is due only to the vertical angle of arrival of the signal and the separation of the two arrays. (Note that there is an additional phase shift associated with the azimuthal angle of arrival of the signal, but this contribution will be ignored for the present discussion.) The predicted phase variation as a function of vertical angle of arrival is shown in Fig. 7. One can see that there is no ambiguity in vertical angle of arrival over the first 35° in elevation angle. This is the range of angles within which we would expect most of the data from both the radar and the communications experiments to lie. Given the accuracies with which the phase angles of the returning signals can be measured, one can expect an accuracy of 1° or better in the determination of the angle of arrival.

A microcomputer at the station controls the radar and processes the incoming data. Two modes of operation are available. In one, an on-site operator enters operating parameters into the microcomputer by means of an on-line display terminal. This mode is used for highly interactive real-time operation of the radar. The other mode is used for noninteractive operation and consists of command strings that are stored on the disk in the form of text files. The strings determine the radar operating times, modes, and frequencies. They may be prepared days or even weeks in advance.

After the relevant radar operating parameters have been entered, radar operation is controlled by a digi-

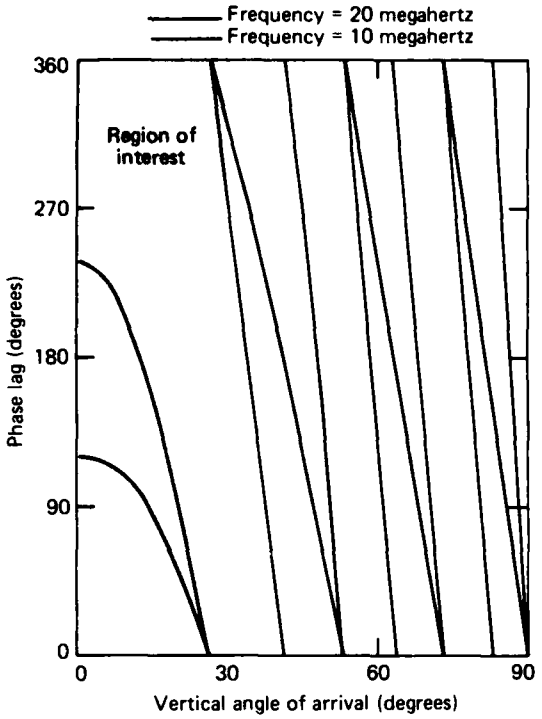

Figure 7—Plot of phase lag as a function of vertical angle of arrival for signals incident on two antenna arrays separated by 100 meters along the direction of propagation. Curves are shown for frequencies of 10 and 20 megahertz.

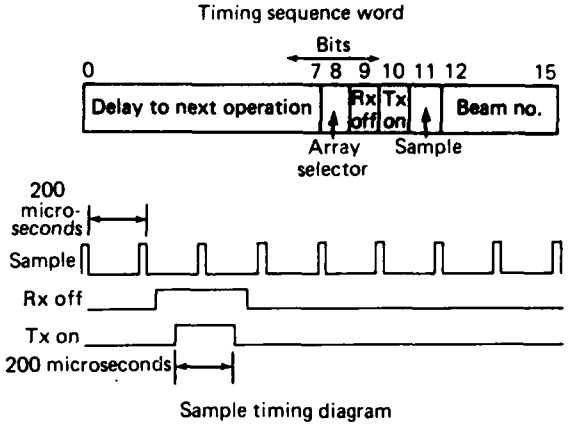

Figure 8—Examples of timing sequencer control word and timing sequence. All time-critical radar functions are under the control of the timing sequencer. This device is a direct-memory-access-controlled buffer that receives 16 bit words from a software-generated timing sequence array within the computer memory. The bits of these control words determine the time delay to the next control word transfer, the antenna array selected, the status of the transmit/receive switch, the status of the transmit pulse, the status of the sample gate, and the antenna beam selected. Generally, the timing sequence is less than 500 words long.

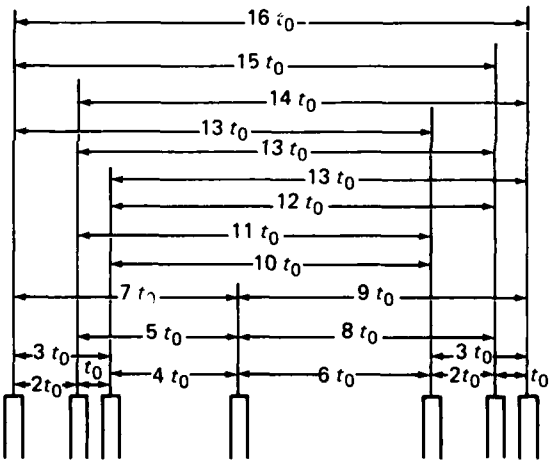

Figure 9—Seven-pulse transmission sequence used for the determination of 17 lag autocorrelation functions of the backscattered signals. From the autocorrelation functions, one can derive the Doppler spectra by Fourier transformation.

tal input-output interface and the timing sequencer. The digital input-output interface is used for non-time-critical operations including frequency selection and receiver gain control. The time-critical operations are controlled by the timing sequencer. This interface receives control words directly from the computer memory via the direct memory access channel of the computer. The words shown in Fig. 8 determine the time to the next control word transfer, the selection of the antenna array, the status of the transmit/receive switch, the status of the radio frequency pulse, the status of the sample gate, and the number of the selected antenna beam. Control words may be transferred every 10 microseconds; however, a more typical interval is 100 to 200 microseconds. Control words are defined by a software subroutine on the basis of the radar operating parameters. In most cases, the length of the control word sequence is about 500 words.

Generally, the control word sequence includes a multipulse transmission of the type shown in Fig. 9. The microcomputer samples the backscattered signals from this seven-pulse pattern and calculates, in real time, 17 lag complex autocorrelation functions (0 to 16 t_0) for a number of distinct ranges. (A seven-pulse sequence is sufficient to yield all the lags for the autocorrelation analysis.) Ideally, each of the lags of the autocorrelation function should occur only once in the sequence because then there can be no ambiguity as to the range of the scattering volume. However, lags t_0, 2 t_0, and 3 t_0 all occur twice, and lag 13 t_0 occurs three times. Fortunately, the time separation between the two occurrences of lags t_0, 2 t_0, and 3 t_0 is so large (39 milliseconds under typical operating conditions) that it is impossible to get simultaneous backscatter from the two sets of pulses. The 13 t_0 lag is a problem, but since there is normally little correlation remaining at these large lags, it has relatively little effect on the total autocorrelation function or on the Doppler spectrum that is derived from it.

As has been noted, the control word sequence determines the sampling of the backscattered signals. Typically, data are obtained from 50 discrete sampling ranges with a spatial separation of 30 kilometers. The

total range interval examined is 1500 kilometers. While data from a given multipulse transmission are being collected, the data from the previous transmission are being processed. Since processing is slightly more time-consuming than acquisition, this radar function ultimately limits the speed of the radar to 10 pattern transmissions per second.

The data from a particular beam direction are accumulated for some predefined integration period (typically 5 to 10 seconds). They are then written onto magnetic tape, and a reduced portion of the available data is plotted on the on-line display. Several plot modes are possible, one of which is shown in Fig. 10. In Fig. 10, the scale across the top line represents the 50 ranges that have been analyzed. The next line presents a gray-scale profile of the backscattered power from each range. If the observed signal-to-noise ratio is less than 3 decibels, no character is plotted. Hyphens are used to represent signal-to-noise-ratio values of 3 to 6 decibels. The following line indicates the mean Doppler velocity of the irregularities at those ranges for which the signal-to-noise-ratio value was greater than 3 decibels. In this case, all the velocities are toward the radar, with higher numbers indicating higher velocities. Finally, the full autocorrelation function is plotted for the range exhibiting the highest signal-to-noise-ratio value. One sees that it is a well-behaved damped sinusoid. The Fourier transform of this function is the Doppler spectrum. For these data, the spectrum will exhibit a mean Doppler velocity of approximately 400 meters per second.

OPERATION OF THE RADAR

Having highlighted some of the principal features of APL's HF radar, let us consider it in operation. By way of example, we will trace through the steps associated with the beam priority operating mode (Fig. 11). Beam priority operation is similar to other radar operating modes in that it is initiated by commands from either the console keyboard or a command file.

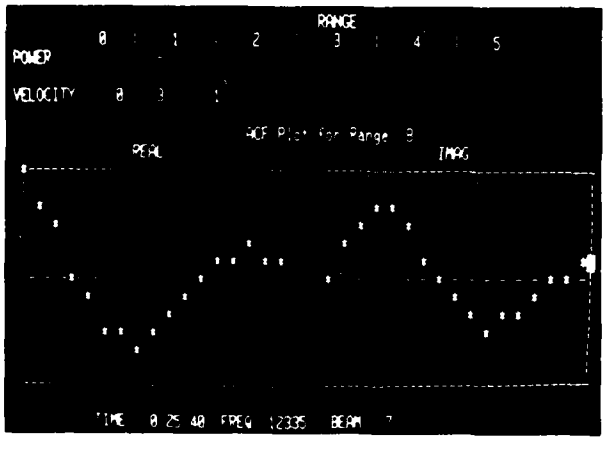

Figure 10—Example of an autocorrelation function of the backscattered signal as plotted on the station on-line display. The autocorrelation function may be plotted for a selected range or for the range with the largest backscattered signal level. Also plotted in the figure are the backscattered power and Doppler profiles of the previous integration. In this example, the signal-to-noise ratio of the signal plotted was in the range of 6 to 9 decibels. (Photograph courtesy of John Kelsey, Canada Marconi.)

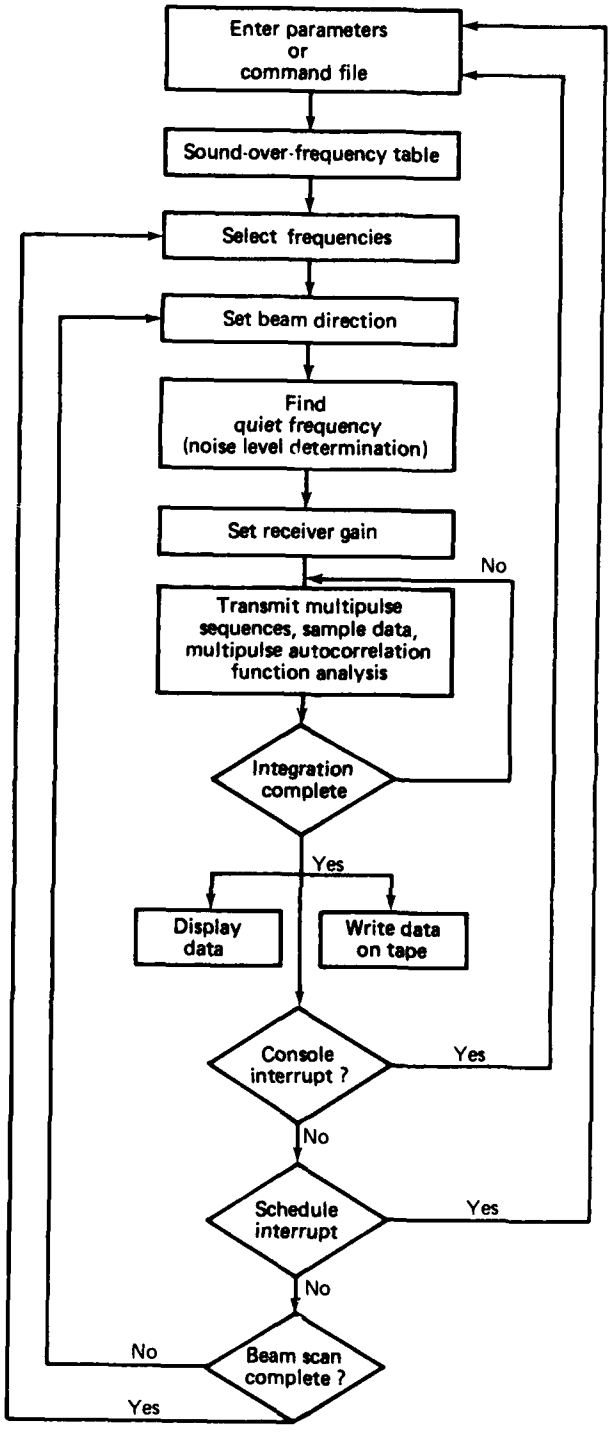

Figure 11—Flow diagram of HF radar operation under the beam priority mode. In this mode, the radar scans through a table of beam directions while operating in a particular 100-kilohertz-wide frequency band. It then proceeds to the next frequency band and repeats the beam scan. It is also possible to have frequency priority operation in which the radar scans through a table of frequencies for each beam direction.

The commands include definition of both the frequency table and the beam table. The former table consists of up to 16 preselected 100-kilohertz frequency bands and the latter of up to 16 beam numbers. Neither table needs to be in any particular order, and the table elements need not be nonrepetitive.

In most cases, the analysis is initiated by an ionospheric sounding over the frequencies contained in the frequency table. This subroutine selects a predetermined number of frequencies for more detailed analysis. The radar then begins with the first selected frequency and proceeds to step through the beam table. For each beam, the radar is first scanned through a 100-kilohertz band centered on the selected frequency in order to determine the quietest 5-kilohertz-wide region within it. This is to ensure the minimum possible disturbance from unwanted signals. The radar then transmits on that frequency, and the receiver gain is adjusted to avoid limiting from strong returns. Next, the radar proceeds with the multipulse analysis for the specified integration time. Upon completion, the data are written onto magnetic tape, and the selected display format is plotted on the video console. A check is made to determine if an interrupt had been generated by either the console or the command schedule. If not, the beam is switched to the next entry in the beam table, or, if the beam scan is complete, the entire scan is repeated at the next selected frequency.

A console interrupt allows new parameters to be entered and the program restarted. A schedule interrupt may cause the program to be temporarily stopped or restarted, or it may reinitiate operation of the sounder subroutine and the selection of new frequencies.

EARLY RESULTS

The APL HF radar has been operating at Goose Bay on a near-daily basis since October 11, 1983, and a wide variety of phenomena has been observed with respect to the formation, dispersal, and decay of F-region irregularities. Here we will present examples of the character and motion of these irregularities as they are observed in the afternoon, late evening, and noon sectors (local time). The order of presentation is related to the increasing complexity of the region being studied.

Afternoon Local Time Sector

The characteristics of high-latitude ionospheric irregularities (i.e., their spatial extent, motion, and possibly their spectral features and mode of formation) are closely related to the local time sectors in which they are observed. In the afternoon sector, there is an east-west aligned boundary that is known as the "convection reversal boundary."[10] The exact geomagnetic latitude of the boundary is dependent on the level of disturbance of the magnetosphere-ionosphere system. For quiet conditions, the boundary may lie at 75°geomagnetic, whereas under disturbed conditions it may lie at 65°. Poleward of the boundary, the plasma moves in an antisunward direction (west-to-east motion), whereas equatorward of the boundary the plasma moves in a sunward direction (east-to-west motion). The boundary also marks the approximate demarcation between polar cap phenomena (poleward of the boundary) and auroral zone phenomena (equatorward of the boundary).

Figures 12a and 12b show examples of the two-dimensional distribution of backscattered power and Doppler velocity from F-region irregularities as they are observed in the afternoon sector. The data were obtained on October 12, 1983, at 2001:32 universal time (UT), approximately 1600 local time. In this example, the irregularities are located equatorward of the convection reversal boundary. The backscattered power distribution has been overlaid on a map of northeastern Canada and Greenland by assuming that the irregularities occur at an altitude of 300 kilometers. (With the installation of the second receiving array, it will no longer be necessary to assume a height for the scattering layer.) Data have been obtained from all 16 beam directions at a frequency of 14.5 megahertz. The irregularities extend across the full east-west

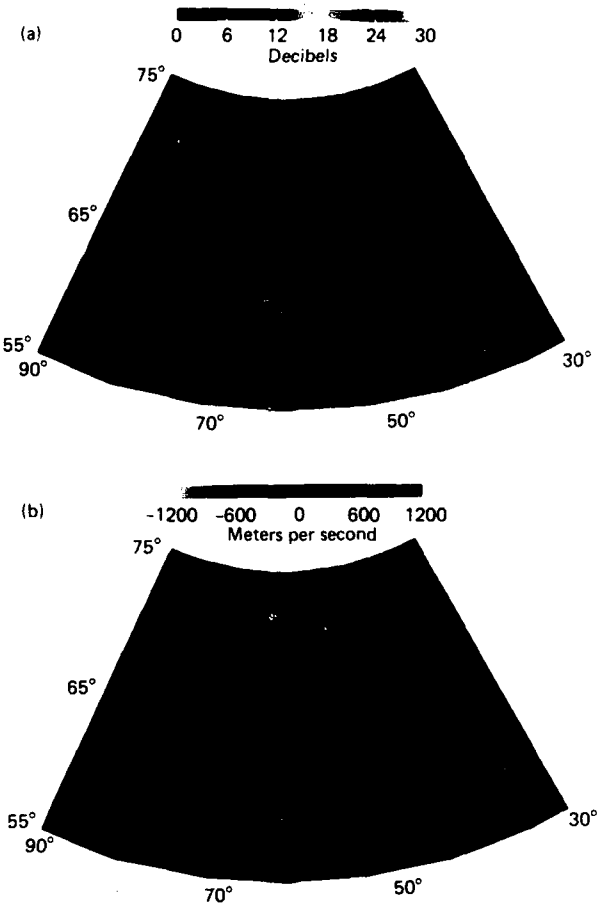

Figure 12—Examples of radar backscattered power (a) and mean Doppler velocity (b) images as obtained on October 12, 1983, at 2001:32 UT at 14.5 megahertz. An intense region of irregularities is located between 900 and 1200 kilometer ranges on all azimuths. The Doppler data indicate that the irregularities are moving on an azimuth of 14° to the south of geographic west at speeds greater than 1600 meters per second. A plan view of northeastern Canada and Greenland is shown in the background.

coverage of the scan (approximately 1000 kilometers) and for about 350 kilometers in range. The structures are extended along a line that is rotated approximately 14° counterclockwise from geographic east-west. The normal to this direction is approximately toward the geomagnetic pole. Closer examination of the backscattered power image reveals a considerable amount of fine structure. Examination of several successive images reveals that this structure is moving along the direction of alignment (slightly south or west) at speeds in excess of 1000 meters per second.

The Doppler velocity data in Fig. 12b also indicate that the irregularities are moving in a direction slightly south of westward. When the radar is directed more toward the east, increasingly positive Doppler velocities are observed, indicating that the irregularity motion is toward the radar, whereas when it is directed more toward the west, the velocities become increasingly negative. One can plot the available Doppler data as a function of azimuth angle and fit them to a cosine curve under the assumption that the radar is measuring the projection of some mean drift velocity. This type of analysis again yields a drift velocity that is directed at an azimuth of approximately 256°. The drift speed obtained from this single-image drift analysis is in excess of 1600 meters per second.

Late Evening Local Time Sector

Near local magnetic midnight, the antisunward plasma flow poleward of the convection reversal boundary emerges from the polar cap and begins to flow sunward by joining either the westward flow in the afternoon auroral zone or the eastward flow in the morning auroral zone (a moment's thought will show that both of these flows are sunward).[10] Our second example of the HF radar data was obtained on October 16, 1983, at 0207:31 UT. It illustrates irregularity structures emerging from the polar cap and moving westward toward the evening sector. The data are shown in Figs. 13a and 13b. One can see from the backscattered power data that the scattering regions are amorphous patches in this local time sector. Their spatial dimensions are typically 100 to 400 kilometers. While it is not obvious from a single image, these patches are actually following a curved trajectory that becomes more westward-directed as the patches move equatorward.

The Doppler data in Fig. 13b are consistent with the trajectory inferred from the backscattered power data. Both patches exhibit positive Doppler values, indicating that they are moving toward the radar and away from the polar cap. However, the poleward patch has a line-of-sight velocity of 700 meters per second, whereas the equatorward patch has a line-of-sight velocity of only 200 meters per second. This reduction is due partially to a slowing of the total irregularity drift velocity after the patch has emerged from the polar cap and partially to a westward rotation of the velocity vector. The rotation causes the equatorward patch to be viewed at a much larger angle relative to its drift direction and leads to a smaller velocity component along the radar line of sight.

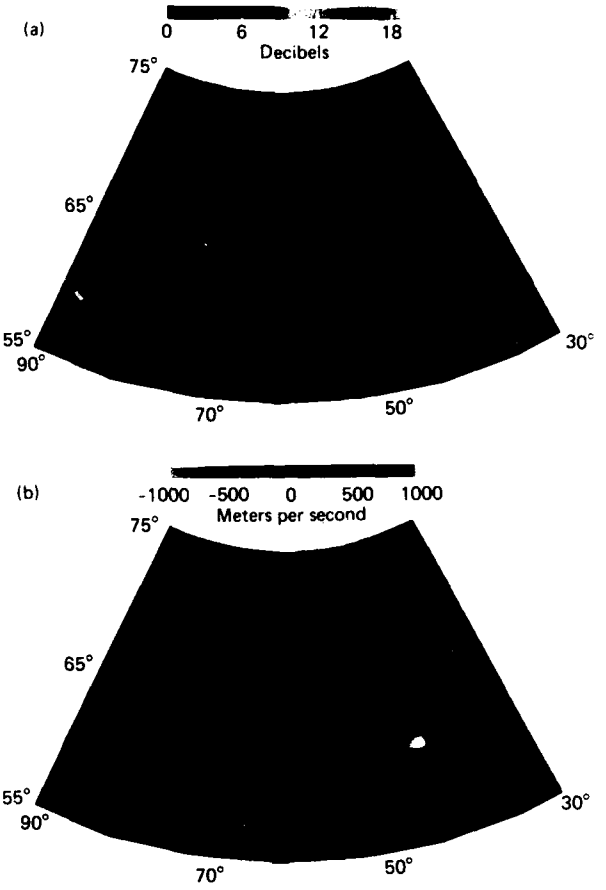

Figure 13—Examples of radar backscattered power (a) and mean Doppler velocity (b) images as obtained on October 16, 1983, at 0207:31 UT at 12.3 megahertz. In this case, the regions of backscatter are more localized amorphous patches that are moving out of the polar cap in a southwesterly direction toward the evening auroral zone.

Noon Local Time Sector

The high-latitude ionospheric plasma motions near local noon are exactly the opposite of those near midnight. In this local time sector and at rather high latitudes (75 to 80° geomagnetic), the sunward-drifting ionospheric plasmas in the late morning and early afternoon sectors (local time) converge and rotate poleward into the polar cap. The exact manner in which this occurs is presently a topic of considerable interest because the magnetic field lines in this region are thought to connect directly to the interplanetary magnetic field. Consequently, the region itself may be strongly affected by the solar wind plasma as well as by the magnitude and direction of the interplanetary magnetic field. The HF radar data that have been selected to represent this local time sector were obtained on November 28, 1983, at 1642:05 UT. The data are of particular interest because they were obtained in conjunction with a passage of the HILAT satellite.

Figures 14a and 14b represent, respectively, the backscattered power and Doppler velocity data for this

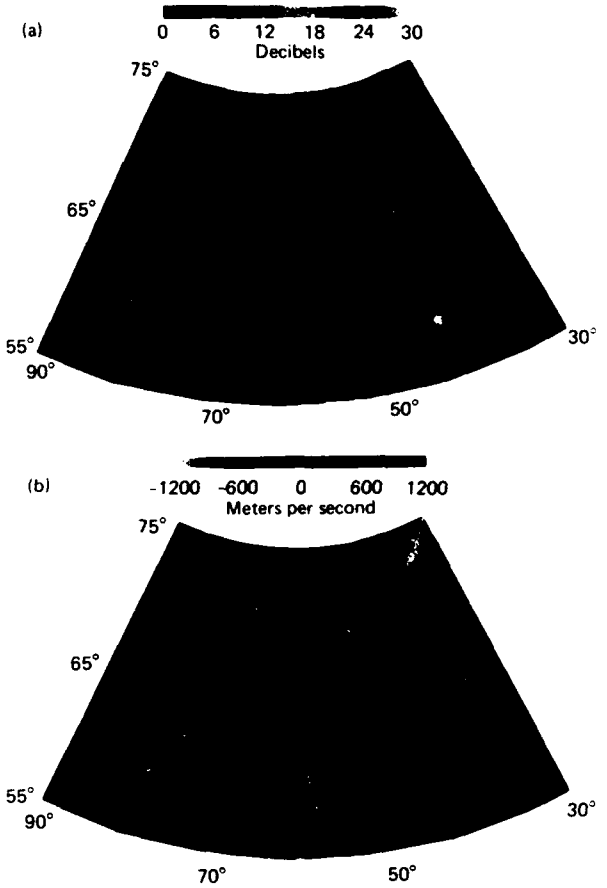

Figure 14—Examples of radar backscattered power (a) and mean Doppler velocity (b) images as obtained on November 28, 1983, at 1642:05 UT at 14.5 megahertz. In this case, the irregularities extend over a number of azimuths; however, the drift is in a northwesterly direction. Also, the drift appears to rotate to a more northerly direction on the western azimuths. The white line represents the line-of-sight path of beacon signals from the HILAT satellite (southwestern end of the line) to a receiving station at Sondre Stromfjord.

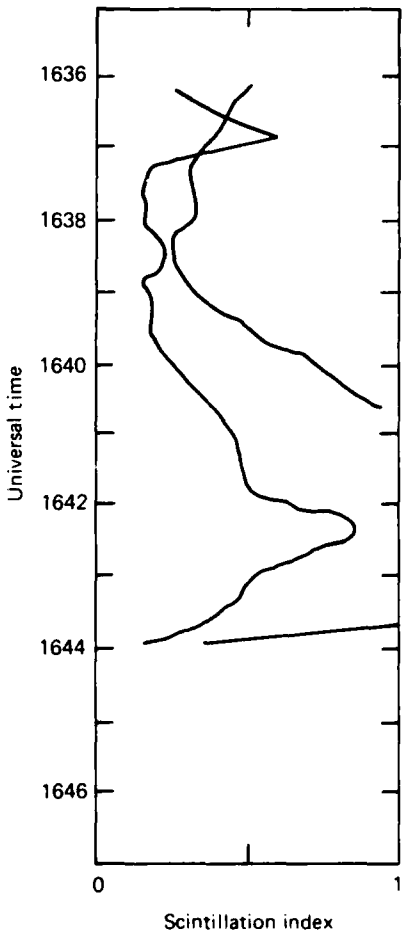

Figure 15—Scintillation index in the HILAT VHF (blue curve) and UHF (red curve) beacon signals as measured at Sondre Stromfjord during the southbound passage of the HILAT satellite (1636 to 1644 UT, November 28, 1983). Note that the maximum scintillation occurred at the time the beacons' ray paths passed through the region of small-scale irregularities.

period. These figures are different from the preceding figures in that they also show the line-of-sight path between the satellite (the western end of the white line) and Sondre Stromfjord. VHF and UHF beacons on board the satellite transmit signals along this path, and the phase and amplitude fluctuations of these signals as observed at Sondre Stromfjord provide a measure of the 100-meter-to-several-kilometer-irregularity structure that exists in the intervening ionosphere. The satellite was moving along a southbound trajectory that carried it from the 85°W meridian in the northern portion of the map to the 75°W meridian at the position shown. Figure 15 shows the beacon scintillation data as they were recorded at Sondre Stromfjord. One sees that the strongest scintillations on both the VHF and UHF beacon signals were observed at 1642 UT, which is the time at which the beacon signals passed through the region of strongest radar backscatter. Thus, there is strong evidence that small- and medium-scale ionospheric irregularities are colocated in space, a result that may be related to the production mechanism of the irregularities.

Although we do not show the data, a drift meter experiment on the satellite indicated that large ionospheric drifts were observed only within a limited region at the approximate latitude of the radar irregularities and that these drifts were directed toward the east. In contrast, careful examination of the Doppler data from the radar indicated that the drift varied from northwestward to northward as the irregularities moved from east to west across the radar field of view. Therefore, it appears likely that these measurements were made at the confluence of the morning and afternoon sunward-directed flow regions.

RADAR APPLICATIONS

The examples of HF radar data shown here represent only brief glimpses of the contributions that the Goose Bay radar may provide to studies of the auroral zone and polar cap ionospheres. While numerous studies of this type are currently in progress, it should

be noted that data obtained with the radar may also have additional value. In particular, they may yield increased insight into the problems that may be encountered by high-latitude HF surveillance systems, and the research effort may indicate possible ways in which these problems can be mitigated. For example, the radar is capable of providing a complete description of the seasonal and diurnal dependencies of irregularity occurrence and spectral characteristics. Since irregularities are a source of clutter on surveillance radar systems, such information would be of particular value for mitigation purposes. Also, the directional capabilities of the antenna array can yield important information on the variability of propagation conditions at high latitudes. Again this information is of importance for proper design and operation of high-latitude HF surveillance systems.

HIGH-LATITUDE PROPAGATION STUDIES

Since the successful installation of the radar at Goose Bay, several federal agencies have supported its use for other applications. Of particular note is a program to study the structure and dynamics of high-latitude communication channels, an effort being sponsored by the electromagnetic and longwave propagation branches of Rome Air Development Center and the Defense Nuclear Agency. At the present time, Rome Air Development Center has installed a 500-watt broadband beacon transmitter at Thule. Signals from this transmitter traverse a 2700-kilometer ionospheric path lying approximately along the 60°W geographic meridian and are received by the antenna array at Goose Bay. Under quiet conditions, there are only one or two possible paths, both lying in the plane of the great circle passing between the stations. However, under disturbed conditions at high latitudes, magnetospheric particle precipitation may produce appreciable F-region structure, as depicted by the elliptical shapes in Fig. 16, and multiple propagation paths may exist. Because this structure is modified continuously by precipitation and is moving at moderately high velocity along with the ambient ionospheric plasma, the number of paths and the modes of propagation are constantly changing. One of the goals of this research effort is to track the variations and interpret them in terms of changing ionospheric configurations. By using both Goose Bay antenna arrays, it will be possible to determine the direction of arrival of the Thule signals with an azimuthal accuracy of 4° and an elevation angle accuracy of 1°. These are very high resolving capabilities for an HF system, and they should provide adequate discrimination of the various propagation channels. Additional resolution is provided by the use of phase-coded signals from Thule. The signals are decoded in real time by the microcomputer at Goose Bay, and, consequently, it is possible to discriminate between signals having similar angles of arrival, provided their path length difference is greater than 60 kilometers over the 2700 kilometers traversed.

The transmissions between Thule and Goose Bay are of two types. First, there is a sounding mode in which

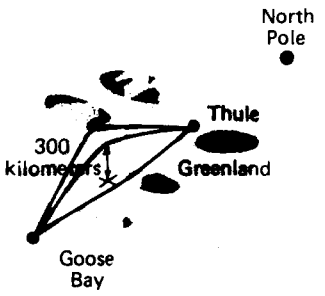

Figure 16—Schematic view of the Thule-Goose Bay propagation experiment showing the manner in which ionospheric electron density enhancements (represented by the shaded regions) produce multipath ionospheric propagation between the two stations.

the Goose Bay antenna is directed toward Thule and both stations scan over the entire 8 to 20 megahertz frequency band. Second, there is a spectral mode in which the Thule beacon transmits repeatedly at specific frequencies and the Goose Bay antenna is scanned over a limited azimuth sector to determine both the angles of arrival and the spectral characteristics of signals reaching Goose Bay along the various propagation channels. Preliminary measurements using the latter mode were begun in April 1984. Figures 17 through 19 illustrate some of the initial results.

Figure 17 represents data obtained on April 17, 1984, at 1205:10 UT. The format of this and the subsequent figures is as follows: Data were obtained from each of eight viewing directions, which are labeled by beam number. Thule lies approximately midway between beams 4 and 5. For each beam direction, 32 phase-coded transmissions were received and decoded at Goose Bay. Each decoded response is plotted vertically along the axis marked relative delay. Zero relative delay corresponds to an absolute delay time of 8 milliseconds and a path length of 2400 kilometers. For each additional millisecond of delay, the path length increases by 300 kilometers. One can see, for example, that the strong signals observed on beams 4 and 5 have propagated over an ionospheric path of 2820 kilometers (9.4 milliseconds). The data are sampled and decoded cyclically over the eight beam directions so that the second sample on beam 1 is obtained after the first sample on beam 8. The results of the 32 samplings, each separated by 25 milliseconds, are plotted horizontally within the box above each beam number. The intensity of the received signal is plotted linearly in terms of signal-to-noise ratio. The noise level selected is the minimum background noise level observed over all of the beam directions.

Several interesting features may be noted from Fig. 17. First, for the relatively quiet ionospheric conditions

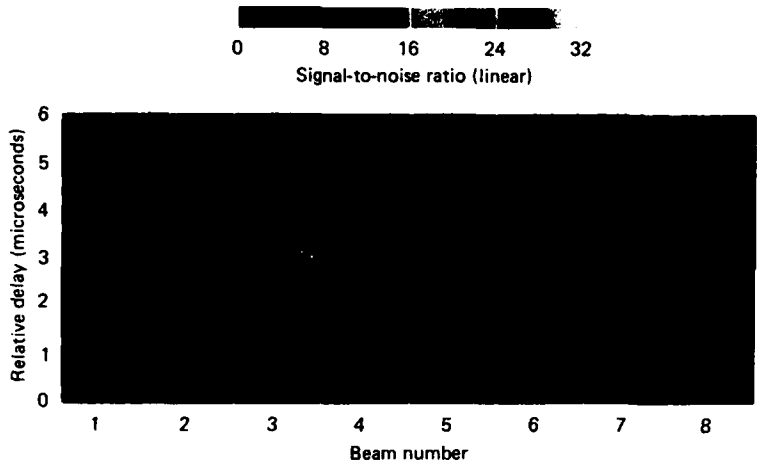

Figure 17—Propagation at 13.39 megahertz between Thule and Goose Bay on April 17, 1984, at 1205:10 UT. The horizontal axis represents data from beams 1 through 8. For each beam direction, 32 samples of data have been obtained. The vertical axis is the decoded relative propagation delay of the signal from Thule. Zero relative delay is an absolute delay of 8 milliseconds and a path length of 2400 kilometers. Each additional millisecond of delay time corresponds to an additional path length of 300 kilometers. Note that signals are predominantly observed on beams 4 and 5, the two azimuths containing Thule within their beam pattern. Strong signals at a relative delay of 1.4 milliseconds and weaker signals at a delay of 1.8 to 2.0 milliseconds are observed.

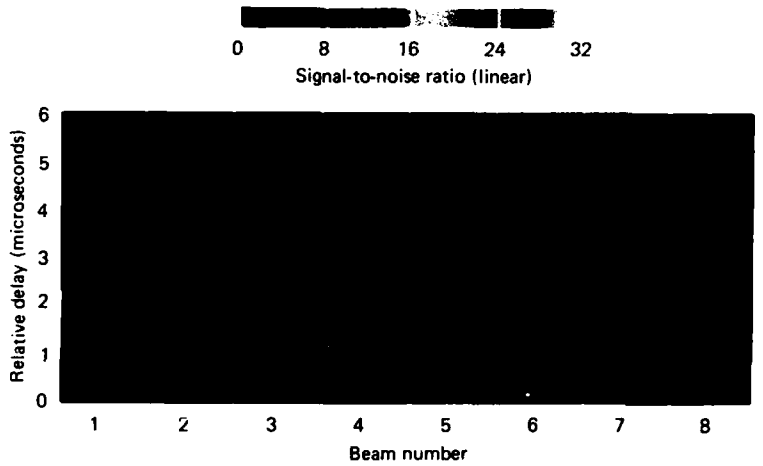

Figure 18—Propagation at 12.30 megahertz between Thule and Goose Bay on April 17, 1984, at 0320:20 UT. Note that at this time, viable propagation paths exist on nearly all beam azimuths, with the strongest signals arriving on beams 3 and 4.

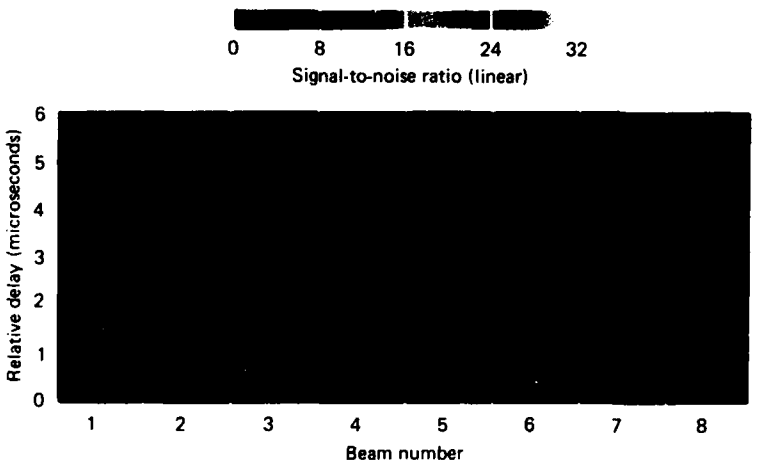

Figure 19—Propagation at 12.30 megahertz between Thule and Goose Bay on April 17, 1984, at 0321:40 UT. These data were obtained 1 minute 20 seconds after the data in Fig. 18. Note that the signals are still arriving on nearly all of the beam azimuths; however, the strongest signals now appear on beams 5 and 6.

that existed at the time of these measurements, propagation was confined to paths that were very close to the direct path. This may be seen by noting that only beams 4 and 5 show significant received power at a relative delay of 1.4 milliseconds. Beams 4 and 5 both show significant power because their beamwidth under receive-only conditions is nearly twice as wide as the angular separation between beams; since their common viewing area includes the direct path toward Thule, one would expect them to yield similar results. The weak signals arriving at a 1.4 millisecond delay on the other beams are most likely due to sidelobes

of these other beams that are pointing in the direction of Thule. Second, there is evidence of an additional path with a relative propagation delay of 1.8 to 2.0 milliseconds. This signal may be associated with the so-called high ray.[11] Propagation by that mode is an additional indication of the nondisturbed nature of the ionosphere. Finally, it is interesting to note that even though the ionosphere does not appear to be disturbed, there is considerable fading of the received signal. Close examination of the temporal variability in the strong signals received on beams 4 and 5 shows power variations by a factor in excess of 30 on time scales of seconds.

Figures 18 and 19 (obtained, respectively, on April 17, 1984, at 0320:20 and 0321:40 UT, shortly before midnight local time) present a marked contrast with the preceding result. In both of these cases, significant power was received over most of the viewing directions. Thus, there appear to have been many ionospheric propagation channels at that time. Moreover, the directions of optimum propagation changed from beams 3 and 4 at 0320:20 UT to beams 5 and 6 at 0321:40 UT. The change may have been due to the motion of ionospheric structure during the intervening time period. Finally, in Fig. 19, it is apparent that the arriving signals have a much greater spread in propagation time than is the case for the daytime data.

Again, the initial results presented here are only a sampling of the potential information that may be gained from this interesting and unique communication experiment. Much can be learned of the finer points of high-latitude propagation, and, possibly, new techniques may be developed to increase the reliability and security of HF communication in a difficult and challenging environment.

SUMMARY

Over the past several years, the HF radar program in the Space Department has grown from a small internal research and development effort into a significant effort that has the support of a number of government sponsors. At the present time, the effort is largely scientific, with a primary goal of obtaining a better understanding of the high-latitude ionosphere and its interactions with the magnetosphere and solar wind. However, it is quite possible that the program will also yield information that may be of considerable value in the design and implementation of future high-latitude HF communications and surveillance systems.

REFERENCES

[1] J. A. Ratcliff, *Sun, Earth and Radio*, McGraw-Hill, New York (1970).

[2] J. V. Evans, "Theory and Practice of Ionosphere Study by Thomson Scatter Radar," *Proc. IEEE* **57**, 496 (1969).

[3] R. A. Greenwald, "Studies of Currents and Electric Fields in the Auroral Zone Ionosphere using Radar Auroral Backscatter," *Dynamics of the Magnetosphere*, S.-I. Akasofu, ed., Reidel, Dordrecht, 213 (1979).

[4] R. T. Tsunoda, R. I. Presnell, and R. L. Leadabrand, "Radar Auroral Echo Characteristics as Seen by the 398-MHz Phased-Array Radar Operated at Homer, Alaska," *J. Geophys. Res.* **79**, 4709 (1974).

[5] K. B. Baker, R. A. Greenwald, and R. T. Tsunoda, "Very High Latitude F-Region Irregularities Observed by HF-Radar Backscatter," *Geophys. Res. Lett.* **10**, 904 (1983).

[6] R. A. Greenwald, K. B. Baker, R. A. Hutchins, and C. Hanuise, "An HF Phased-Array Radar for Studying Small-Scale Structure in the High Latitude Ionosphere," *Radio Sci.* **20**, 63 (1985).

[7] G. C. Reid, "The Formation of Small-Scale Irregularities in the Ionosphere," *J. Geophys. Res.* **73**, 1627 (1968).

[8] D. T. Farley, "A Plasma Instability Resulting in Field-Aligned Irregularities in the Ionosphere," *J. Geophys. Res.* **68**, 6083 (1963).

[9] S. L. Ossakow and P. K. Chaturvedi, "Current Convective Instability in the Diffuse Aurora," *Geophys. Res. Lett.* **6**, 332 (1979).

[10] R. A. Heelis and W. B. Hanson, "High-Latitude Convection in the Nighttime F-Region," *J. Geophys. Res.* **85**, 1995 (1980).

[11] J. M. Kelso, *Radio Ray Propagation in the Ionosphere*, McGraw-Hill, New York (1964).

ACKNOWLEDGMENTS—It is important to acknowledge the many individuals who have participated in the development of the Goose Bay HF radar facility. These include APL staff members: K. B. Baker, R. A. Hutchins, S. Bouldin, H. P. Von Gunten, A. W. Bennett, G. Palmer, and the Electronic Fabrication Group; M. Mandelberg, J. Waaramaa, R. Galik, K. Degen, R. Gowel, and J. Winterbottom of the Air Force Geophysics Laboratory; J. Kelsey, W. Conkie, and B. Gill of Canada Marconi; C. Hanuise of LSEET, University of Toulon, France; M. Pinnock of the British Antarctic Survey; and R. Drake and T. Sevenson of the U.S. Air Force.

Support for the radar has been provided by the APL IR&D Program, the National Science Foundation (Grant ATM-8216571), the Air Force Office of Scientific Research, the Defense Nuclear Agency, the Air Force Geophysics Laboratory, and the Rome Air Development Center.

THE AUTHOR

RAYMOND A. GREENWALD was born in Chicago in 1942. He received an undergraduate degree from Knox College and a Ph.D. degree in physics from Dartmouth College in 1970, specializing in laboratory plasma physics. After completing a postdoctoral fellowship studying laboratory plasmas at the National Oceanic and Atmospheric Administration/Environmental Research Laboratory Aeronomy Laboratory in Boulder, Colo., he continued working there, using ground-based radars to study plasma instabilities in the ionosphere.

In 1975, Dr. Greenwald moved with his family to Lindau, West Germany, where he worked for the Max-Planck Institut für Aeronomie. There, he led the development of the STARE radars, which have been used during the past eight years to study plasma processes in the ionosphere over northern Scandinavia.

In 1979, Dr. Greenwald and his family returned to the United States, and he joined the staff of APL. Since then, he has been involved in several radar and satellite research programs. Most recently, he has led the development of the APL high-frequency radar at Goose Bay, Labrador, which is being used to study both high-latitude ionospheric irregularity formation and high-latitude electromagnetic propagation.

Dr. Greenwald is a section supervisor in the Space Physics Group of the APL Space Department.

In the photo, he is fastening an anchor onto one of the radar antennas.

END

FEB.

1988

DTIC